THERMAL MODEL FOR ELECTROMAGNETIC LAUNCHERS

H. Zhao,

J. A. Souza,

and J. C. Ordonez

Department of Mechanical Engineering,

and Center for Advanced Power Systems

Florida State University, Tallahassee, FL

32310, USA

ABSTRACT

This paper presents a 3D model for the determination of the temperature field in an electromagnetic launcher. The large amounts of energy that are dissipated into the structure of an electromagnetic launcher during short periods of time lead to a complicated thermal management situation. Effective thermal management strategies are necessary in order to maintain temperatures under acceptable limits. This paper constitutes an attempt to determine the temperature response of the launcher. A complete three-dimensional model has been developed. It combines rigid body movement, electromagnetic effects and heat diffusion together. The launcher consists of two parallel rectangular rails and an armature moving between them. Preliminary results show the current distribution on the rail cross-section, the localized resistive heating, and the rail transient temperature response. The simulation results are compared to prior work presented for a 2D geometry by Powell and Zielinski (2008).

Keywords: Electromagnetic launcher, Resistive heating, Thermal Management, Numerical simulation.

NOMENCLATURE

$\vec{A}$	vector magnetic potential, Wb/m	
$\vec{B}$	magnetic flux density, T	
c_p	specific heat, kJ/kg·K	
$\vec{D}$	electric flux density, C/m^2	
$\vec{E}$	electric field intensity, V/m^3	
$\vec{F}$	Lorentz force acting on the armature, N	
F_x	x-component of the Lorentz Force, N	
$\vec{J}$	current density, A/m^2	
$\vec{J}_e$	externally generated current density, A/m^2	
$\vec{J}_0$	input current, A/m^2	
k	thermal conductivity, W/m·K	
M	armature mass, kg	
$\vec{n}$	normal vector	
t	time, s	
T	temperature, K	
V	electrical potential, V	
x_0	armature position, m	

Greek symbols

μ	permeability, H/m	
ρ	density, kg/m^3	
ρ_v	volume charge density, C/m^3	
σ	conductivity, S/m	
Ω	armature volume, m^3	

INTRODUCTION

The cooling of an electromagnetic launcher constitutes a challenging thermal management problem. High heat fluxes of pulsating nature result as a consequence of its operation. Large amount of energy (of the order of $10^1 – 10^2$ MJ) is deposited in the launcher structure in periods that last a few milliseconds.

From the heat transfer point of view, the problem is interesting not only because of the high heat pulses, but also because of the coupled physical phenomena behind the large energy dissipation. The model should account for the movement of the projectile, the imposed current, the associated magnetic field and the temperature gradient resulting from the ohmic dissipation. Another aspect that makes this problem attractive is its non-uniformity; the current density the ohmic resistance and associated heat generation are not distributed uniformly throughout the rail cross section, instead a "skin" phenomena occurs leading to a concentration of current and heat generation in the outer layers of the rail (Marshall, 1984)

In recent years, much effort has been focused on the development and improvement of electromagnetic launcher technology. The design parameters placed on the railguns by the U.S. Navy are 300~500 km range and continuous firing rate of up to 12 shots per minute (McFarland and McNab, 2003). The practical limitation of the barrel length is between 10~12 m. These requirements lead to high current levels (about 6 MA) and short pulse duration

(about 8 ms). About 16% of the total energy (Smith et al., 2007) will be deposited in the launcher structure. This high energy deposition makes the thermal management an important issue. Several recent numerical investigations have been performed to study the electromagnetic field and heat generation (Powell et al., 1993; Powel and Zielinski, 1995; Smith at al., 2005) in electromagnetic launchers.

In this paper, a full three-dimensional model is used to simulate the launching process. The 20 kg projectile (embedded in an armature) is accelerated from rest to about 2000 m/s in 8 ms. The trajectory of the projectile, current transport in the rails and the transient temperature response are computed.

MODEL

A sketch of the computational model is shown in Fig.1. The launcher is represented by two parallel rails and a moving armature. The surrounding air is included to account for the magnetic field and the "magnetic insulation" boundary condition (see Eq. (16)).
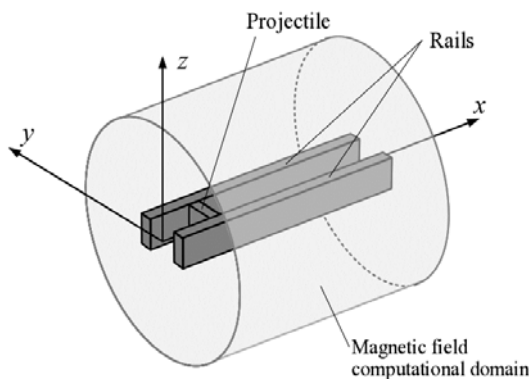
Figure 1. Schematic representation of the computational domain.

The material of the rails is copper and the armature is made of aluminum. The dimensions of the rail and the armature are 12 m x 0.06 m x 0.135 m and 0.04 m x 0.135 m x 0.135 m (length x width x height). Table 1 gives other properties for the rail and armature.

Table 1. Properties of the rail and armature

Property	Unit	Rail (Copper)	Armature (Aluminum)
ρ	kg/m^3	8700	
k	W/m.K	400	
σ	S/m	5.98×10^7	3.77×10^7
c_p	J/kg.K	385	

Fig. 2 and Fig. 3 are the 2-D projection of the railgun in horizontal and vertical directions. From Fig. 2 we can see that the driving current flows through one rail, across the armature and then flows

back along the other rail. In the current model, a fixed mesh is used and the armature movement is modeled as a moving conductor distribution that is interpolated on the fixed mesh.
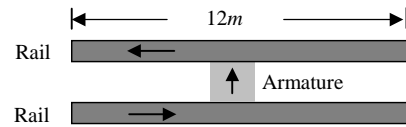
Figure 2. Top view of the launcher.
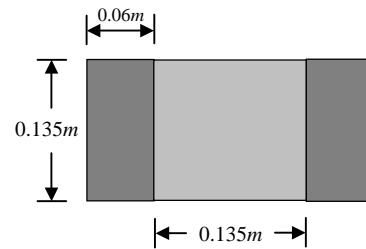
Figure 3. Vertical cross section of rails and armature.

The equations to be solved are the appropriate Maxwell's equations, the energy transport equation for the rails, and an equation to account for the moving armature.

Let μ and σ be the permeability and the electric conductivity, $\vec{E}, \vec{D}, \vec{B}, \vec{J}$ and ρ_v be the electric field density, the electric flux density, the magnetic flux density, the current density and volume charge density. The governing Maxwell's equations are as follows:

$$\nabla \times (\frac{1}{\mu} \vec{B}) = \vec{J} \tag{1}$$

$$\nabla \times \vec{E} = -\frac{\partial \vec{B}}{\partial t} \tag{2}$$

$$\vec{J} = \sigma(\vec{E} + \vec{v} \times \vec{B}) + \vec{J}_e \tag{3}$$

$$\nabla \cdot \vec{D} = \rho_v \tag{4}$$

$$\nabla \cdot \vec{J} = -\frac{\partial \rho_v}{\partial t} \tag{5}$$

In Eq. (1), the displacement current $\partial \vec{D}/\partial t$ is neglected (Powel at al., 1993). By taking the time derivative on both sides of Eq. (4) we obtain $\partial \rho_v/\partial t = 0$. Then Eq.(5) can be simplified to Eq.(6).

In Eq. (3) $\vec{J}_e$ is an externally generated current density to specify all source currents and $\vec{v}$ is the velocity of the moving conductor.

$$\nabla \cdot \vec{J} = 0 \qquad (6)$$

Let V and $\vec{A}$ be the scalar electric potential and the vector magnetic potential, respectively. Then we have,

$$\vec{E} = -\nabla V - \frac{\partial \vec{A}}{\partial t} \qquad (7)$$

$$\vec{B} = \nabla \times \vec{A} \qquad (8)$$

By combining Eqs. (1), (3), (7) and (8), an expression for the vector magnetic potential is obtained.

$$\sigma \frac{\partial \vec{A}}{\partial t} + \nabla \times (\frac{1}{\mu}\nabla \times \vec{A}) - \sigma \vec{v} \times (\nabla \times \vec{A}) + \sigma \nabla V = \vec{J}_e \qquad (9)$$

And if we make a further approximation by neglecting the coupling between electric and magnetic field that is neglecting induced currents $\partial \vec{B}/\partial t$ from Eq. (2), we get $\nabla \times \vec{E} = 0$, which means that the electric field can be expressed in terms of electric potential as shown in Eq. (10). This approximation holds when the skin depth is much larger than the geometry of the conductor. For our specific input current J_0, this condition is satisfied.

$$\vec{E} = -\nabla V \qquad (10)$$

By applying the same approximation in Eq. (3) it is possible to obtain Eq. (11). Combining Eqs. (6), (10) and (11) we obtain Eq. (12) for current balance.

$$\vec{J} = \sigma \vec{E} + \vec{J}_e \qquad (11)$$

$$\nabla \cdot (\sigma \nabla V - \vec{J}_e) = 0 \qquad (12)$$

The energy equation is represented in (13). The source term is given by $\vec{J} \cdot \vec{J}/\sigma$. In this study, the resistive heating in the armature is neglected. So Eq. (13) is only solved in the rails.

$$\rho c_p \frac{\partial T}{\partial t} = \nabla \cdot (-k\nabla T) + \frac{\vec{J} \cdot \vec{J}}{\sigma} \qquad (13)$$

Finally we consider the armature's movement. Let M and F_x be the mass of the armature and the Lorentz force acting on the armature along the rail direction. The Lorentz force can be calculated through formula (14). Ω is the volume of the armature.

$$\vec{F} = \int_\Omega \vec{J} \times \vec{B} d\Omega \qquad (14)$$

The dynamic equation for the armature position x_0 is:

$$\frac{d^2 x_0}{dt^2} = \frac{F_x}{M} \qquad (15)$$

Equations (9), (12), (13) and (15) are the basic differential equations to be solved subject to some set of appropriate initial and boundary conditions. The dependent variables for these four equations are $\vec{A}, V, T$ and x_0.

MODEL VERIFICATION

The present model is first compared with a two-dimensional study by Powell and Zielinski (2008) (see Figs. 5-8).

The two-dimensional model is shown in Fig. 4. The computational domain is one quadrant (left-top part) of the configuration shown due to symmetry about *y=0* and vertical center line. The assumptions for this 2-D problem are (Powell and Zielinski, 2008): (1) $\vec{A} = A\hat{k}, \vec{E} = E\hat{k}, \vec{J} = J\hat{k}$ and (2) all variables depend only on x and y and not on z.
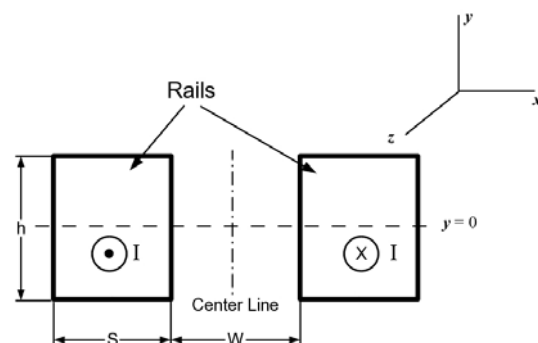
Figure 4. x-y cross section of the rails.

In Powell and Zielinski's (2008) work, a 2D form of Eq. (9) is used. However the current balance equation (Eq. (11)) is not solved.

Starting from assumption (1), it is possible to write $\vec{J}_e = J_e\hat{k}$ and $\nabla V = \nabla V\hat{k}$ from Eqs. (7) and

(11). By substituting $J_e \hat{k}$ and $\nabla V \hat{k}$ into Eq. (12), and using the assumption (2), Eq. (12) is then satisfied automatically. Under these two assumptions, the formalisms for the electromagnetic (EM) field for this and the Powell and Zielinski's (2008) work are identical. The energy equation is also the same.

By setting the identical boundary conditions expressed in Eqs. (16) and (18), we can verify the current model with results from Powell and Zielinski's (2008). Fig. 5 and Fig. 7 were taken from Powell and Zielinski's (2008) and Fig.6 and Fig. 8 are the present model results. These figures validate, in a qualitative way, the solution obtained with the present model. A quantitative validation was not possible since only graphical information is available in the work of Powell and Zielinski's (2008).

Fig. 5 shows the solution obtained by Powell and Zielinski's (2008) for the magnetic potential field. This figure is compared with Fig. 6 obtained with the present solution. A qualitative analysis shows that the gradients in both figures are similar and that the maximum values for the magnetic potential are in good agreement.
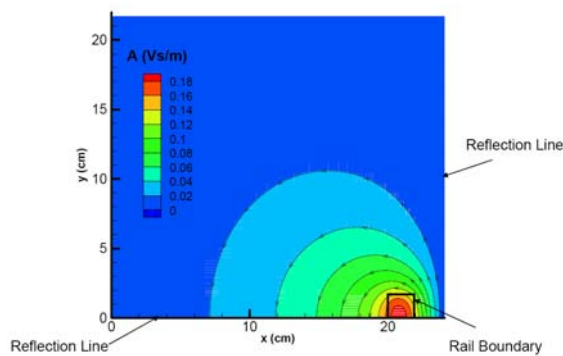
Figure 5. Magnetic potential contours at 5 ms (Powell and Zielinski's, 2008).
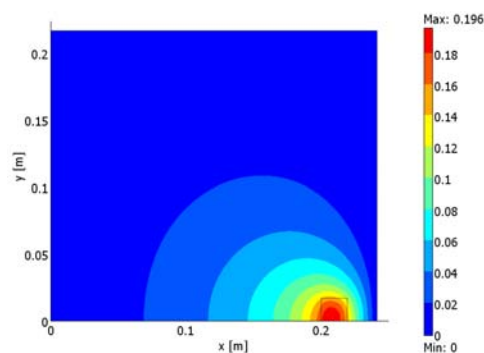
Figure 6. Magnetic potential contours at 5 ms.

In Figs. 7 and 8 the temperature fields are compared. The maximum temperature is 365 K in

both solutions, and the location of the hot spot is in both cases the upper right corner. The gradients and temperature values are qualitatively similar. Note that color scale is different from Fig. 7
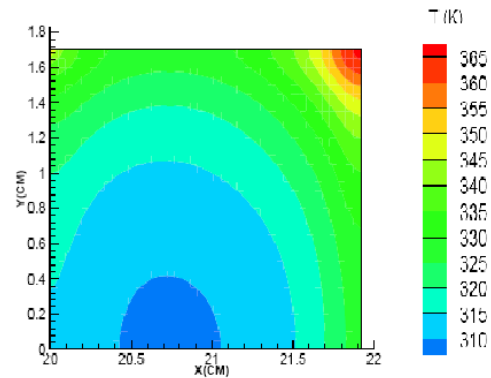
Figure 7. Rail temperature response at 5 ms (Powell and Zielinski's, 2008).
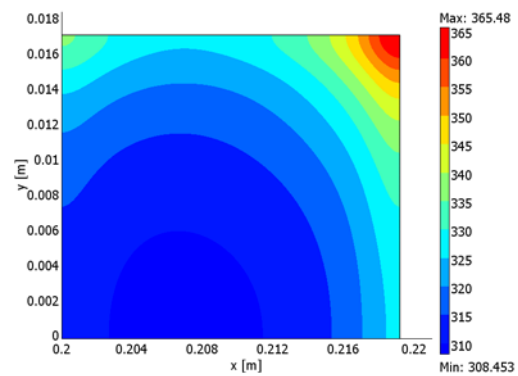
Figure 8. Rail temperature response at 5 ms.

3D CASE STUDY

The model discussed in the previous sections is now extended to the 3D problem schematically represented in Fig. 1. The problem's boundary conditions are discussed in the following section.

Boundary Conditions

For the magnetic field the "magnetic insulation" condition on $\vec{A}$ at each exterior boundary which sets the tangential component of magnetic potential to zero is used. Here, $\vec{n}$ represents the outward normal direction of any exterior surface. Eq. (16) shows this boundary condition for Eq. (9).

The "electric insulation" condition, Eq.(17), is applied on external boundaries except for the two current driven ends of the rails. And the condition $\vec{J} = \vec{J}_0$ and $V = 0$ are set for the two ends

respectively. In this study, $\vec{J}_0$ is considered uniform on the boundary.

For the energy equation, a thermal insulation condition, Eq. (18), is set on all rail surfaces.

$$\vec{n} \times \vec{A} = 0 \tag{16}$$

$$\vec{n} \cdot \vec{J} = 0 \tag{17}$$

$$\vec{n} \cdot \nabla T = 0 \tag{18}$$

Initial Conditions

$$\begin{aligned}
\vec{A} &= 0 \quad Wb/m \\
V &= 0 \quad V \\
T &= 300K \\
x_0 &= 0 \quad m \\
dx_0/dt &= 0 \quad m/s
\end{aligned} \tag{19}$$

Equations (9), (12), (13) and (15) with the indicated boundary and initial conditions are solved simultaneously to determine the electromagnetic field, temperature response in the rails and the position and velocity of armature.

Numerical Results

The specific input current $\vec{J}_0$ used in this study is shown in Fig. 9.
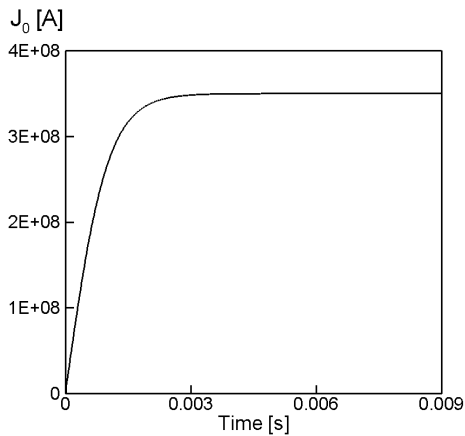
Figure 9. Input Current J_0.

Figure 10 illustrates the position of the armature during launching.
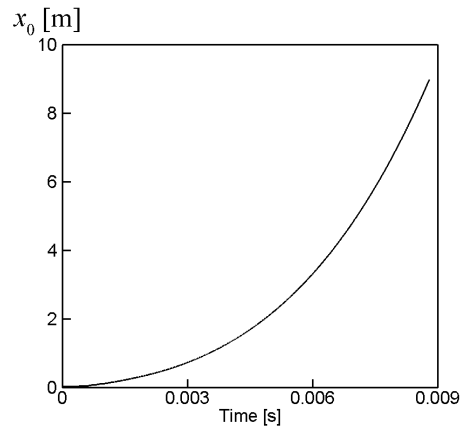
Figure10. Armature position x_0.

Figure 11 shows the armature velocity.
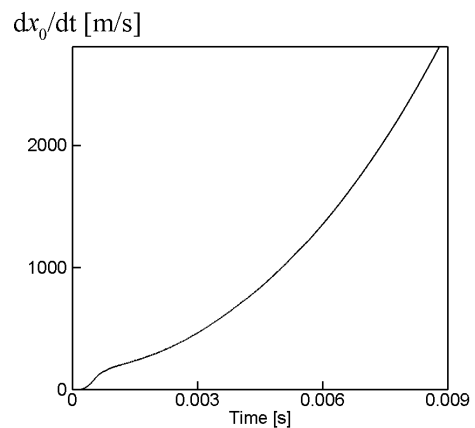
Figure 11. Armature velocity dx_0/dt .

The maximum temperature of the rail varies with time, as shown in Fig. 12.
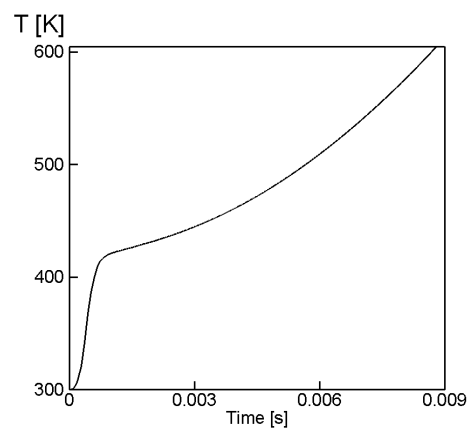
Figure12. Maximum temperature of the rail during launching.

Figs. 13 and 14 show the temperature and current profile of a cross-section (at x = 4m, t = 0.0088s) of the rail. From these two figures, we can see that the temperature and current have similar distributions. The current distribution qualitatively matches the results by Kerrisk (1981).
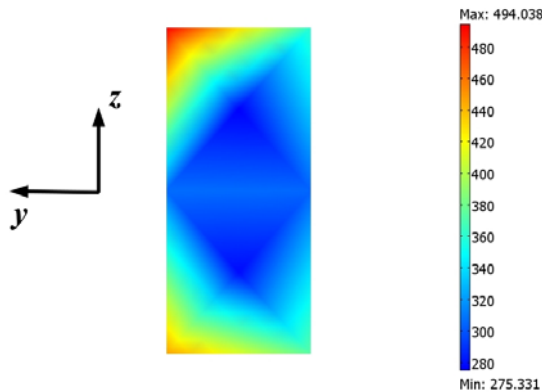
Figure 13. Temperature profile at $x = 4$ m and $t = 0.0088$ s.
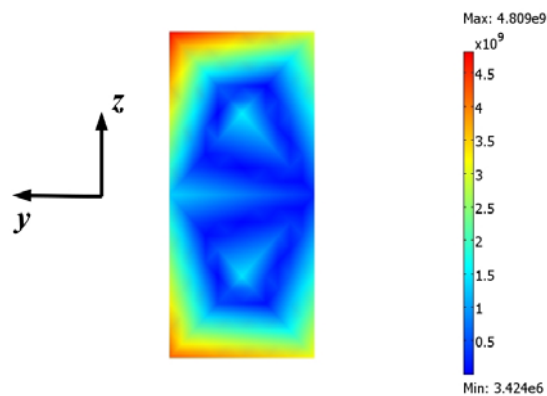
Figure 14. Current profile at $x = 4$ m and $t = 0.0088$ s.

CONCLUSION

A full three dimensional model is presented to simulate the launching process of an electromagnetic launcher. The solution was first validated by comparison with available results of a 2D problem (Powel and Zielinski, 2008). After validation, a complete 3D problem, with coupled magnetic and thermal phenomena, was solved. At this first step, the relationship between temperature and current density was investigated. In a follow up work, cooling channels will be added to the model in order to study the best geometric configuration of the rails cooling system.

Since the temperature profile on a cross-section shows that the inside edge has the highest temperature. It is expected that the cooling channels should be located closer to the inside face of the rail.

However, its exact location and form are aspects to be investigated.

REFERENCES

COMSOL Multiphysics Inc., 2005, User's Manual, Los Angeles, CA.

J. F. Kerrisk, 1981, Current Distribution and Inductance Calculations for Railgun Conductors, Los Alamos Tech. Rep. LA-9092-MS, Nov.

Marshall, R. A., 1984, Current Flow Patterns in Railgun Rails, IEEE Transactions on Magnetics, Vol. 20, No. 2, pp. 243-244.

McFarland, J., and McNab, I. R., 2003, A Long-Range Naval Railgun, IEEE Transactions on Magnetics, Vol. 39, pp. 289-294.

Powel, J. D., and Zielinski, A. E., 1995, Current and Heat Transport in The Solid-Armature Railguns, IEEE Transactions on Magnetics, Vol. 31, pp. 645-650.

Powell, J. D., and Zielinski, A. E., 2008, Two-Dimensional Current Diffusion in the Rails of a Railgun, Army Research Laboratory, ARL-TR-4618.

Powell, J. D., Walbert, D. J. and Zielinski, A. E., 1993, Two-Dimensional Model for Current and Heat Transport in Solid-Armature RaSilguns, US Army Research Laboratory Report Number ARL-TR-74.

Smith, A. N., Ellis, R. L., Bernardes, J. S. and Zielinski, A. E., 2005, Thermal Management and Resistive Rail Heating of a Large-Scale Naval Electromagnetic Launcher, IEEE Transactions on Magnetics, Vol. 41, No. 1.

Smith, A. N., McGlasson, B. T., and Bernardes, J. S., 2007, Heat Generation During the Firing of a Capacitor-Based Railgun System, IEEE Transactions on Magnetics, Vol. 43, No. 1.

Zielinski, A. E., Niles, S., and Powell, J. D., 1999, Current and Heat Conduction during a Pulsed Electrical Discharge, Journal of Applied Physics, Vol. 86, pp. 3943-3952.